Paper: ASAT-14-207-IP

14th International Conference on
AEROSPACE SCIENCES & AVIATION TECHNOLOGY,
ASAT - 14 – May 24 - 26, 2011, Email: asat@mtc.edu.eg
Military Technical College, Kobry Elkobbah, Cairo, Egypt
Tel: +(202) 24025292 –24036138, Fax: +(202) 22621908

Performance Evaluation of Range Image Segmentation Based on Surface Fitting Method

A. Maher*, H. Taha†, F. Eltohamy‡, M. Mamdouh†

Abstract: In this paper, range images edge-based segmentation is investigated. The edge detection in the range images is based on calculating significant change in the angle between surfaces normal by computing the surface normal in 3D for each point in the image. Three methods for computing surface normal based on different Surface Fitting are considered. First one is the Eigenvector Method (EM), and second is the Weighted Least Squares Method (WLSM) which is achieved by combining both Eigenvector and least square methods (LSM), finally the Least Median of Squares method (LMS). These segmentation methods have been applied on 3 test range images of polyhedral objects [1], using Matlab under Linux operating system. Following the process of segmentation, a performance evaluation of the applied segmentation methods is done. Experimental results show that significant performance improvement of range image segmentation by LMS method can be achieved.

Keywords: Range image, segmentation, surface fitting, EM, WLSM, LMS

1. Introduction

The process of information extraction from an image is known as image analysis. The first step in image analysis is the image segmentation [2]. Simply it is the operation at the threshold between low-level image processing and image analysis. As a result, an image is segmented (classified) into a set of homogeneous and meaningful regions or objects, where each image pixel should belongs to an object. Once an image is segmented, the next task is to recognize the segmented objects or regions. Algorithms for range image segmentation falls into two basic categories: 1) region-based or 2) edge-based. There are also the so called hybrid techniques that use both region and edge information to guide the segmentation process. In [4] range image segmentation algorithms were analyzed. One of the major conclusion of this analysis is that range image segmentation is still not really a solved problem even for simple scenes containing only polyhedral objects. The main problem is that in most algorithms, it is difficult to accurately detect at the same time geometric surfaces and exact edge locations between those surfaces.

In his paper the investigated algorithms are edge-based. The framework followed in this work is shown in the block diagram, Fig. 1. Starting with smoothing the image in order to suppress noise and obtain the smoothed range image R_m by using median filter. Next Edge-based segmentation for detecting objects boundaries is applied, where the fitting parameters affecting the process of edge detection using EM, WLSM and LMS are investigated. In range

* Egyptian Armed Forces, Email: ali_mtc@hotmail.com
† Egyptian Armed Forces, Egypt.
‡ Egyptian Armed Forces, Email: ftohamy72@yahoo.com

images there are different kinds of discontinuities that can be mainly classified as depth ("step edges") which refers to abrupt change in range value (depth) of the original image and roof ("crease edges") which refers to changes in the normal vector orientation. The process of edge detection followed by morphological operations, where the thinning and filling (connectivity) of detected edges and back ground removal are performed, then the labeling of connected components (regions) is performed. Finally the performance evaluation of the applied fitting parameters method is done.

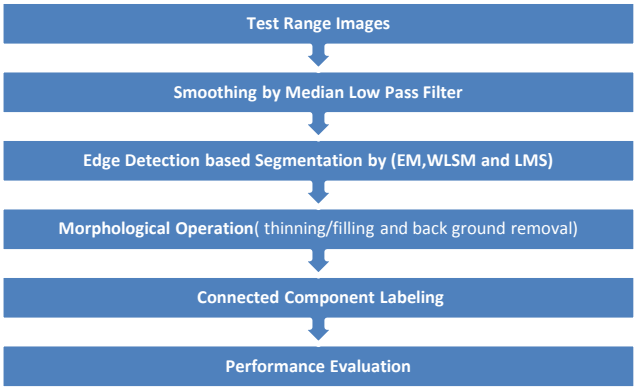

Fig. 1 Framework block diagram

2. Test Images

For this work a database of 40 images, acquired with a laser range finder (LRF) scanner which uses a single optical path and computes depth via the phase shift or time delay of a reflected laser beam. The LRF produces range images of size 512 × 512 with 12 bits per pixel was used, varying from (0 to 4095) gray level. The database was made available for free by the University of South Florida. All the objects in this database are polyhedral. Every range image has a ground truth (GT) image associated with the range one for the comparison with the results of segmented images. Figure 1 gives three samples test images from the data base, one with single object, second with two objects and the third with five occluded objects.

Single object **Double objects** Multi objects

Fig. 2 Selected three test range images from the database.

3. Range Image Segmentation

Generally the methods of range image segmentation fall into two basic categories [4]:

1. Region-based segmentation methods (homogeneity): which group range pixels into connected regions based on some similarity measure. Typically, they grow regions around seed points for which a planar fit gives a reliable estimate.

2. Edge-based segmentation approaches (discontinuity) which locates boundaries between regions by finding points of discontinuity from the range image and then used to guide the segmentation process.

There is also a third approach called hybrid techniques that use both region and edge information to guide the segmentation process.
Any of these approaches has its strength and weaknesses and can need an extensive post-processing phase. For example, Edge-based approach tends to produce thick edges and gaps in the boundaries of the regions. There for it should be followed by thinning and filling (connectivity) operations.

Generally the segmentation algorithm that segments an image represent by set R into distinct n subsets, R_1, R_2, ... R_n, this process should satisfy the following 5 conditions [13, 14]:

1. $\bigcup_{i=1}^{n} \boldsymbol{R_i} = \boldsymbol{R}$, This condition means that the segmentation process is terminated when every pixel is assigned to a region, or a subset.
2. $\boldsymbol{R_i}$ is a connected region for i =1, 2,...,n, This condition means that the pixels of a region should be connected (i.e. satisfy the conditions of connectivity).
3. $\boldsymbol{R_i} \cap \boldsymbol{R_j} = \emptyset$ for all i and j, where $i \neq j$, this condition means that the subsets (regions) should be disjoint.
4. $\boldsymbol{P}(\boldsymbol{R_i}) = TRUE$ for i =1, 2,..., n, This condition means that the property must be satisfied by the pixels of a segmented region.
5. ($\boldsymbol{P}.\boldsymbol{R_i} \cup \boldsymbol{R_j}$) = FALSE for i=1,2,...,n. This condition means that the region $\boldsymbol{R_i}$and $\boldsymbol{R_j}$are different in the sense of the property P.

3.1 Range Image Edge-Based Segmentation

In this work edge based segmentation for detecting object boundaries is applied using EM, WLSM and LMS. Let R_m is the smoothed range image after applying the median filter. Next, the step edge magnitude, denoted by E_{step} is obtained as the maximum difference in depth between a point (r,c) and its neighbors (r+k, c+l) as follows:

$$E_{\text{step}}(r,c) = \max_{k,l \in w} \left\{ \left| R_m(r,c) - R_m(r+k, c+l) \right| \right\} \tag{1}$$

where R_m (r,c) is the depth value, and w is the window size used to find the step edge.
Then a threshold operation is used to decide if (r,c) is a point on a step edge or not. Finding step edges is considered easier than detecting roof edges. Most edge detection methods [5] can detect step edges.
Roof edges can be detected by measuring the significant change in the angle between surface normal by fitting the data. Some works which use Eigenvector, least squares and Weighted Least Squares methods in fitting range data are published [6, 7 and 8].

3.2 Fitting Plane Procedures

Briefly we will discuss the difference between the EM, LSM, WLSM and LMS in fitting range data and their efficiency for detecting roof edges.

3.2.1 Best fitting plane in case of eigenvector method (EM)

Range data consist of n measurements {x_i, y_i and z_i where i= l, 2 ...n}, for planar surface the best fitting plane in case of Eigenvector method is given by [8]:

$$\boldsymbol{ax + by + cz = d} \tag{2}$$

where *a*, *b*, *c* and *d* satisfy the following two conditions.

$$a^2 + b^2 + c^2 = 1 \tag{3}$$

and

$$d \geq 0 \tag{4}$$

Then the distance of the i[th] point to the plane without regard to sign is given by

$$d = \{(ax_i + by_i + cz_i) - (ax_p + by_p + cz_p)\} \tag{5}$$

where (x_p, y_p, z_p) is any point on the best fit plane and (x_i, y_i, z_i) is any point on the plane. The triplet (*a*, *b*, *c*) denotes the direction cosines of any perpendicular drawn on the plane pointing away from the origin of the coordinate system. Equivalently, it denotes the components of the unit normal vector drawn on the plane pointing away from the origin; *d* denotes the perpendicular distance between the plane and the origin.
The second term of RHS is the distance from the origin to the best fitting plane, and the first term is the distance from origin to another plane parallel to the former and passing through the i_{th} data point. According to the least square method the best fitting plane is the plane which minimizes the non-negative quantity D^2 ,in (6), with respect to *a*, *b* and *c*.

$$D^2 \equiv \sum_{i=1}^{n} d_i^2 \tag{6}$$

However, *a*, *b* and *c* cannot vary freely; if they could, then the result would be $a = b = c = 0$, and $D_2 = 0$, this will contradict with constraint given in (3).

The point (x_c, y_c, z_c) is the "center of mass" of the data points which already lies on the best fitting plane, even before the direction cosines *a*, *b*, *c* and the distance *d* that minimize the above sum are determined. This point is given by:

$$\begin{aligned} x_c &= \frac{1}{\mathrm{n}\sum_{\mathrm{i}=1}^{\mathrm{n}} x_i} \\ y_c &= \frac{1}{n\sum_{i=1}^{n} y_i} \\ z_c &= \frac{1}{n\sum_{i=1}^{n} z_i} \end{aligned} \tag{7}$$

Since the best fit plane should pass through this point, so we should to minimize the value of Q defined by:

$$\boldsymbol{Q} = \sum_{\mathrm{i}=1}^{\mathrm{n}} \mathrm{d}_\mathrm{i}^2 = \sum_{\boldsymbol{i=1}}^{\boldsymbol{n}} \{ (\boldsymbol{ax_i + by_i + cz_i}) - (\boldsymbol{ax_c + by_c + cz_c})\}^{\boldsymbol{2}} \tag{8}$$

By differentiating $\boldsymbol{Q}$ with respect to *a*, *b* and *c* and equating the result to zero we have the following:

$$\begin{aligned} \frac{\boldsymbol{dQ}}{\boldsymbol{da}} &= \sum_{\boldsymbol{i=1}}^{\boldsymbol{n}} \{\boldsymbol{a}\,(\boldsymbol{x_i - x_c})^{\boldsymbol{2}} + \boldsymbol{b}(\boldsymbol{y_i - y_c})(\boldsymbol{x_i - x_c}) + \boldsymbol{c}(\boldsymbol{z_i - z_c})(\boldsymbol{x_i - x_c})\} \\ \frac{\boldsymbol{dQ}}{\boldsymbol{db}} &= \sum_{\boldsymbol{i=1}}^{\boldsymbol{n}} \{\boldsymbol{a}\,(\boldsymbol{x_i - x_c})(\boldsymbol{y_i - y_c}) + \boldsymbol{b}(\boldsymbol{y_i - y_c})^{\boldsymbol{2}} + \boldsymbol{c}(\boldsymbol{y_i - y_c})(\boldsymbol{z_i - z_c})\} \\ \frac{\boldsymbol{dQ}}{\boldsymbol{dc}} &= \sum_{\boldsymbol{i=1}}^{\boldsymbol{n}} \{\boldsymbol{a}\,(\boldsymbol{x_i - x_c})(\boldsymbol{z_i - xz_c}) + \boldsymbol{b}(\boldsymbol{y_i - y_c})(\boldsymbol{z_i - z_c}) + \boldsymbol{c}(\boldsymbol{z_i - z_c})^{\boldsymbol{2}}\} \end{aligned} \tag{9}$$

Let,

$$\Delta \mathrm{x} = (\boldsymbol{x_i - x_c}),\ \Delta \boldsymbol{y} = (\boldsymbol{y_i - y_c}), \Delta \boldsymbol{z} = (\boldsymbol{z_i - z_c}) \tag{10}$$

In linear differential equation homogenous system we have:

$$Q' = AQ \tag{11}$$

To construct a general solution to (11), we assume a solution of the form $Q = Vert$, where the exponent r and the constant vector V are to be determined.
Substituting $Q = Vert$ into (11), we obtain:

$$rVe^{rt} = \mathbf{A}Ve^{rt} \quad \Leftrightarrow \quad rV = \mathbf{A}V \quad \Leftrightarrow \quad (\mathbf{A} - r\mathbf{I})V = \mathbf{0} \tag{12}$$

Thus to solve the homogeneous system of differential equations Q' = AQ, we can find the eigenvalues and eigenvectors of **A** as follows:

$$\begin{bmatrix} \sum \Delta x \Delta x & \sum \Delta y \Delta x & \sum \Delta z \Delta x \\ \sum \Delta x \Delta y & \sum \Delta y \Delta y & \sum \Delta z \Delta y \\ \sum \Delta x \Delta z & \sum \Delta y \Delta z & \sum \Delta z \Delta z \end{bmatrix} \begin{bmatrix} a \\ b \\ c \end{bmatrix} = \lambda \begin{bmatrix} a \\ b \\ c \end{bmatrix} \tag{13}$$

A is a real symmetric matrix; it must have three real eigenvalues λ_k and three corresponding normalized eigenvectors $[a_k \quad b_k \quad c_k]^T$, where k= 1,2,3. Multiplying (13) by $[a_k \quad b_k \quad c_k]$ from left we obtain :

$$[a_k \quad b_k \quad c_k] \begin{bmatrix} \sum \Delta x \Delta x & \sum \Delta y \Delta x & \sum \Delta z \Delta x \\ \sum \Delta x \Delta y & \sum \Delta y \Delta y & \sum \Delta z \Delta y \\ \sum \Delta x \Delta z & \sum \Delta y \Delta z & \sum \Delta z \Delta z \end{bmatrix} \begin{bmatrix} a_k \\ b_k \\ c_k \end{bmatrix} = [a_k \quad b_k \quad c_k] \lambda_k \begin{bmatrix} a_k \\ b_k \\ c_k \end{bmatrix} \tag{14}$$

But

$$[a_k \quad b_k \quad c_k] \begin{bmatrix} a_k \\ b_k \\ c_k \end{bmatrix} = 1 \tag{15}$$

Then

$$\lambda_k = \sum_{i=1}^{n} (a\Delta x_{ic} + b\Delta y_{ic} + c\Delta z_{ic})^2 = \sum_{i=1}^{n} d_i^2 \tag{16}$$

Equation (16) proves that the eigenvalues of Q are non-negative, and the minimum value of $\sum_{i=1}^{n} d_i^2$ equals the lowest eigenvalue. The corresponding eigenvector determines the parameters *a*, *b* and *c* of the best fit plane. But d can be determined by the fact that center of mass point lies on that plane, and computed as $d=ax_c+by_c+cz_c$.

3 2.2 Best fitting plane in case of least squares method (LSM)

The Eigenvector method of finding the best fit plane is more general than the least squares method [8]. It will be seen that the former method assumes that all measured variables contain error. But in (LSM) only one variable contains error (*z*), this is the dependent variable. All other variables are independent variables(*x*, *y*) which are assumed to contain no or negligible error. The least squares problem in these situations is relatively simple where the best fit plane to a set of points is given by:

$$z = f(x, y; p, q, r) = p + qx + ry) \tag{17}$$

where *p*, *q* and *r* are the parameters which will be found by the least squares procedure.
So if independent variables have values x_i and y_i then the measured value of *z* should be $p+qx_i+ry_i$. However, the measured value of *z* is z_i, then the error in the i^{th} measurement is then

$$\boldsymbol{e_i = f(x_i, y_i; p, q, r) - z_i} \tag{18}$$

According to the least squares method, *p*, *q* and *r* are to be chosen such that to minimize the following sum of the squares:

$$\boldsymbol{E^2 = \sum_{i=1}^{n} e_i^2 = \sum_{i=1}^{n} (p + q x_i + r y_i - z_i)^2} \tag{19}$$

Differentiating equation (19) with respect to parameters *p*, *q* and *r* and put each derivative equal to zero, we get three equations which can be combined in matrix form as follow:

$$\begin{bmatrix} \boldsymbol{n} & \boldsymbol{\sum x_i} & \boldsymbol{\sum y_i} \\ \boldsymbol{\sum x_i} & \boldsymbol{\sum x_i^2} & \boldsymbol{\sum x_i y_i} \\ \boldsymbol{\sum y_i} & \boldsymbol{\sum x_i y_i} & \boldsymbol{\sum y_i^2} \end{bmatrix} \begin{bmatrix} \boldsymbol{p} \\ \boldsymbol{q} \\ \boldsymbol{r} \end{bmatrix} = \begin{bmatrix} \boldsymbol{\sum z_i} \\ \boldsymbol{\sum z_i x_i} \\ \boldsymbol{\sum y_i z_i} \end{bmatrix} \tag{20}$$

This leads to evaluate *p*, *q* and *r* for (LSM) method.

3.2.3 Best fitting plane in case of weighted least squares method (WLSM)

$\mathrm{n_{EM}} = (\mathrm{a}, \mathrm{b}, \mathrm{c})$ is (EM) normal vector and for the (LSM) normal vector is given by $\mathrm{n_{LSM}} = (-\mathrm{q}, -\mathrm{r}, 1)$ [9]. The unit surface normal $\hat{n}$ is obtained by dividing the surface normal by its length.

$$\hat{n_{EM}} = n_{EM} = (a, b, c) \tag{21}$$

$$\hat{n_{LSM}} = \frac{(-q, -r, 1)}{\sqrt{q^2 + r^2 + 1}} \tag{22}$$

From the unit normal definitions we can conclude that

$$\mathrm{a} = -\mathrm{qc}, \mathrm{b} = -\mathrm{rc}\,, \mathrm{d} = \mathrm{cp} \tag{23}$$

$$|c| = \frac{1}{\sqrt{q^2 + r^2 + 1}} \tag{24}$$

Since the range data contain noise (each variable has error), so we cannot use the usual least squares method to find the parameters of two planes making up the roof, therefore the EM can be used. However the investigation about the uncertainties in the best fit parameters *a*, *b*, *c* and *d* of the EM is not easy to do [8]. So a combination of the eigenvector method and the usual least squares method (called Weighted Least Squares Method-WLSM) can be applied to find the parameters. EM is used to find d_i (the distance of each point from the plane) then by dividing (Weighting) each e_{i2} in (19) by d_{i2} to get (25). Using these weights, one can proceed through the weighted least squares to obtain *p*, *q* and *r* through (26, 27) and then we get unit normal for each point from (22).

$$E^2 = \sum_{i=1}^{n} \frac{e_i^2}{d_i^2} = \sum_{i=1}^{n} \omega_i e_i^2 \tag{25}$$

$$\begin{bmatrix} \sum \omega_i & \sum \omega_i x_i & \sum \omega_i\ y_i \\ \sum \omega_i x_i & \sum \omega_i x_i^2 & \sum \omega_i x_i y_i \\ \sum \omega_i y_i & \sum \omega_i x_i y_i & \sum \omega_i y_i^2 \end{bmatrix} \begin{bmatrix} \mathrm{p} \\ \mathrm{q} \\ \mathrm{r} \end{bmatrix} = \begin{bmatrix} \sum \omega_i z_i \\ \sum \omega_i z_i x_i \\ \sum \omega_i y_i z_i \end{bmatrix} \tag{26}$$

$$\begin{bmatrix} p \\ q \\ r \end{bmatrix} = E_w \begin{bmatrix} \sum \omega_i z_i \\ \sum \omega_i z_i x_i \\ \sum \omega_i y_i z_i \end{bmatrix} \tag{27}$$

where $\boldsymbol{E_w}$ stands for the inverse of the modified 3x3 matrix in (26).
Best fitting plane in case of least median of squares (LMS)
Simply, (LSM) fits the plane by finding the parameters that minimize the sum of squared residuals (SSR), which are represented in (19).
Generally we have two types of data clean (without outliers) and bad (with extreme values) data, least squares would perform well if a clean data is used. Therefore performing an enhancement operation on range data by median filter before edge detection by (LSM) is crucial and will affect the performance of (LSM).
Smallest percentage of bad data that can cause the fitted plane to explode is defined as the breakdown points, Least squares performs poorly in terms of robustness because a single, aberrant range data point, or outlier, can affect the values of the fitting parameters, and then gives large residual error.
LMS is a less sensitive, or more robust, fitting technique than least squares. It should come as no surprise that an estimator using the median would be less sensitive to extreme values than conventional least squares, which is related to the average. The median of the list {1, 2, 3} is the same as the median of the list {1, 2, 100}, while the averages are quite different. An example associated with using least squares on dirty data is given in [11].
By noting that minimizing the sum of squared residuals is equivalent to minimizing the mean of the squared residuals. Dividing the SSR by the number of observations will give the average of the squared residuals without changing the minimum [10].

$$\begin{aligned} &\underbrace{\boldsymbol{min}}_{\boldsymbol{p,q,r}} \boldsymbol{SSR} = \textstyle\sum_{i=1}^{n} (\boldsymbol{p + qx_i + ry_i - z_i})^2 \\ Or \quad &\underbrace{\boldsymbol{min}}_{\boldsymbol{p,q,r}} \textbf{Average SSR} = \frac{1}{\mathbf{n}} \textstyle\sum_{i=1}^{n} (\boldsymbol{p + qx_i + ry_i - z_i})^2 \end{aligned} \tag{28}$$

As Rousseeuw [12] pointed out, "Most people have tried to make these estimators robust by replacing the square by something else, why not, however, replace the sum by a median, which is very robust?" Formally, the Least Median of Squares fit is determined by solving the following optimization problem (29)

$$\begin{aligned} \underbrace{\boldsymbol{min}}_{\boldsymbol{p,q,r}} \boldsymbol{mid_i\, SR} = \boldsymbol{Median}\{&(\boldsymbol{p + qx_1 + ry_1 - z_1})^2, (\boldsymbol{p + qx_2 + ry_2 - z_2})^2, \\ &\ldots (\boldsymbol{p + qx_n + ry_n - z_n})^2\} \end{aligned} \tag{29}$$

The solution leads to estimate planar surface parameters p, q and r and going through (22) to evaluate the unit surface normal $\boldsymbol{n}^{\wedge}$.

4. Computer Work and Comparison Methodology

4.1 Computer Work

The selected three range images of Fig. 2 are processed according to the following algorithm:

- A window (*W*) of size 15×15 surrounding each image point is chosen for fitting plane
- Normal vectors are calculated at each image point using EM, WLSM and LMS
- The angles between all pairs of surface normal vectors are computed,

- Next, the maximum angle E_{roof} between surface normal vectors at locations (r, c) and ($r+k$, $c+l$) is computed as follows [5]:

$$E_{\text{roof}} = \max_{k,l \in w} \left\{ \cos^{-1}\left(\hat{n}(r,c) \cdot \hat{n}(r+k, c+l)\right) \right\} \tag{30}$$

- If $E_{roof} > T_{roof}$, where T_{roof} is an empirically determined threshold, then (r, c) is assumed to lie on a roof edge.

The previous algorithm is applied over the three selected test range images, Fig. 2, using Matlab software under Linux operating system. The results are given in Fig. 3.

(EM) method Edge Map (a)

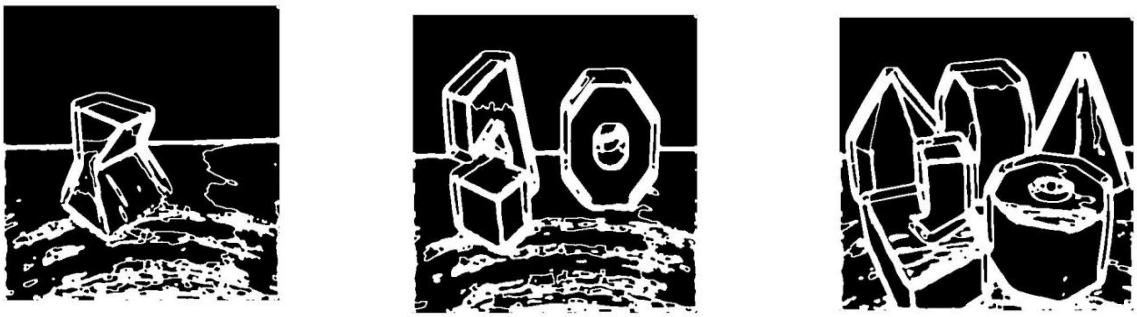

(WLSM) method Edge Map (b)

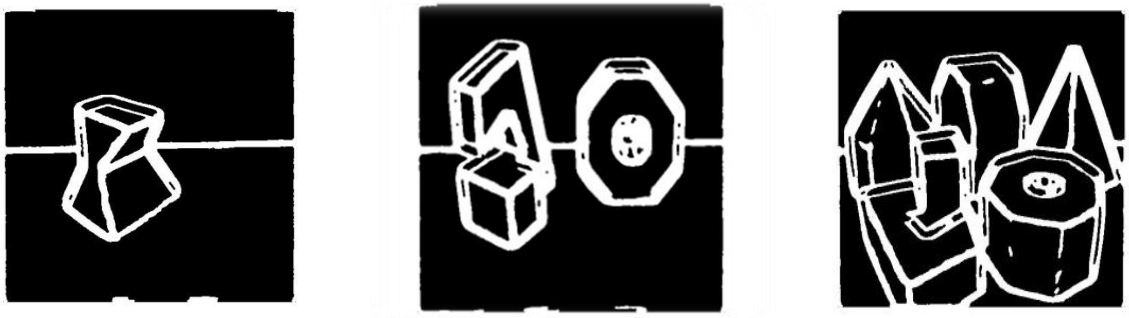

(LMS) method Edge Map (c)

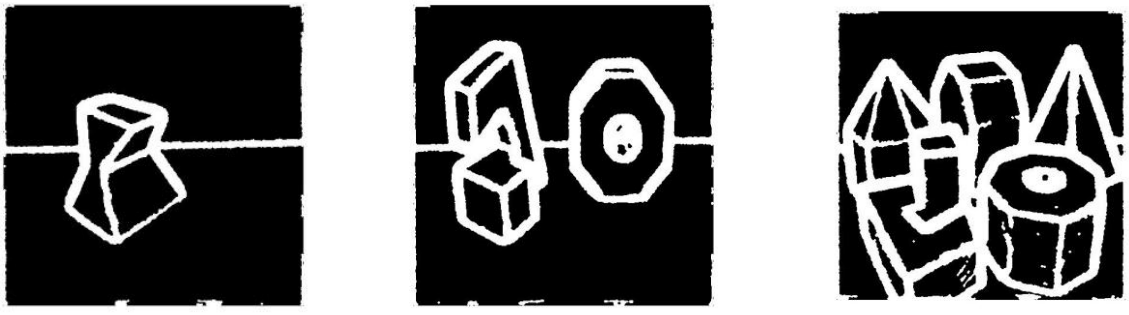

Fig. 3 Illustration of different edge maps according to different normal vector calculation. (a) Edge map using EM. (b) Edge map using WLSM (c) Edge map using LMS.

4.2 Performance Measures

This section introduces briefly the methodology [4] used to compare the performance of the three implemented segmentation algorithms. The comparison between the automatic segmentation (Machine Segmentation, *MS*) and the manual segmentation (Ground Truth Segmentation, *GT*) were performed as follows [15]: Let M be the number of regions in the *MS* image, and N the number of regions in the *GT* image. Let P_m be the number of pixels in the *MS* region R_m (where $m = 1...M$). In the same way, let P_n be the number of pixels in the *GT* region R_n (where $n = 1...N$). Let $O_{mn} = R_m \cap R_n$ be the number of pixels that simultaneously belongs to regions R_m and R_n. According to this definition, we find $O_{mn} = 0$, if there is no overlap between regions, and $O_{mn} = P_m = P_n$. in the case of complete overlap.

Then, it is possible to build the $M \times X\ N$ table, with the O_{mn} values, for $m=1...M$ and $n = 1...N$. This result will be used to calculate the overlapping index for every region in the MS image as (O_{mn}/P_m and in the *GT* image as O_{mn}/P_n).These indexes provide the discriminate information to classify every segmented region as one of five classes: *Correct Detection, Over-Segmentation, Under-Segmentation, Missed and Noise*, Fig. 4.

Over-Segmentation refers to a multiple detection of a single surface. Under-Segmentation refers to a merge of surfaces into a single one. A Missed occurs when the segmentation algorithm is not successful in the detection of a surface that appears in the image, and Noise occurs when the algorithm detects a surface that is not present in the image.

The equations to classify every surface uses a threshold T, in the interval $0.5 < T \leq 1.0$. The value of T is determined by:

1. Correct Detection. Two regions, R_m in the *MS* image and R_n in the *GT* image are classified as a Correct Detection if:
   a. $Omn \geq T \times P_m$ (at least T percent of the pixels in R_m of the *MS* image, are marked as belonging to R_n in the *GT* image), and
   b. $O_{mn} \geq T \times P_n$ (at least T percent of the pixels in R_n of the *GT* image, are marked as belonging to R_m in the *MS* image).
2. Over-Segmentation. One region R_n in the *GT* image and a set of regions R_{m1}, R_{mx} in the *MS* image, where $2 \leq x \leq M$, are classified as an instance of Over-Segmentation if:
   a. $\forall\ i \in x,\ O_{min} \geq T \times P_m$ (for all i, at least T percent of the pixels in each region R_{mi} of the *MS* image also belong to R_n in the *GT* image), and
   b. $\sum_{i=1}^{x} \boldsymbol{O_{min}} \geq T \times P_n$ (at least T percent of the pixels of R_n in the *GT* image also belong to the union of the regions $R_{m1},...,R_{mx}$ in the *MS* image).
3. Sub-Segmentation. Given a set of regions $R_{n1},...,R_{nx}$, $2 \leq x \leq M$, in a *GT* image, then one region R_m in an *MS* image is classified as an instance of Sub-Segmentation if:
   a. $\sum_{i=1}^{x} \boldsymbol{O_{mni}} \geq T \times P_m$ (at least T percent of the pixels in R_m of the *MS* image, also belong to the union of regions R_{n1}, R_{nx} in the *GT* image), and
   b. $\forall i \in x,\ O_{mn} \geq T \times P_m$ (at least T percent of the pixels in R_{ni} of the *GT* image also belong to R_m in the *MS* image).
4. Missed. A region R_n of the *GT* image that is not classified as an instance of Correct Detection, Over-Segmentation or Under-Segmentation is classified as Missed.
5. Noise. A region R_m of the *MS* image that is not classified as an instance of Correct Detection, Over-Segmentation or Under-Segmentation is classified as Noise.

Even though these indexes produce a classification for every surface in the images *GT* and *MS*, this classification is not unique for $T < 1.0$. Furthermore, for the range $0.5 < T < 1.0$,

every region can eventually contribute to three categories (Correct Detection, Over-Segmentation or Under-Segmentation). In the case more than one definition is satisfied, the region is classified according to the maximum index.
The "perfect" segmentation algorithm should be able to correctly detect all the regions with tolerance 1.0, and without instances of Over-Segmentation, Under-Segmentation, Missed or Noise.

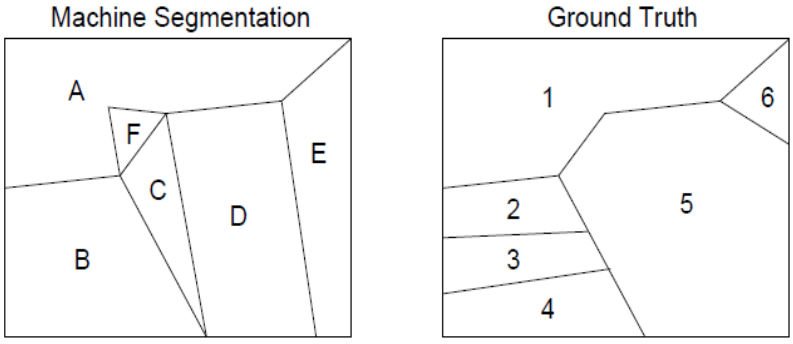

Fig. 4 MS region A corresponds to GTS region 1 as an instance of correct segmentation, GT region 5 corresponds to MS regions C, D, and E as an instance of over-segmentation, MS region B corresponds to GT regions 2, 3, and 4 as an instance of under-segmentation, GT region 6 is an instance of a missed region, MS region F is an instance of a noise region.

5. Results

The result of the complete segmentation process performance on test image of a single object Fig. 2a is shown in Fig. 5a, while Fig. 5b shows the corresponding the ground truth image

(a) (b)

Fig. 5 (a) LMS Segmentation result, (b) Ground Truth

In the previous comparison methodology, section 4.2 used to determine the performance of each method, it is essential to notice that for applied segmentation techniques, special treatment was needed for the background planes. There are some considerations that need to be taken into account in order to perform a good comparison. That the two regions (back ground) are considerable bigger than the regions under analysis. This can make a wrong understanding of the performance indexes and consequently as are classified as "Correct Detection" even for highly restrictive values of the tolerance parameter *T*. Therefore the background was removed and we only used images with a single object in the scene [15].

Figure 6 presents the percentage of Correct Detection for performance of each segmentation methods which demonstrate how the regression methods affect the segmentation process.

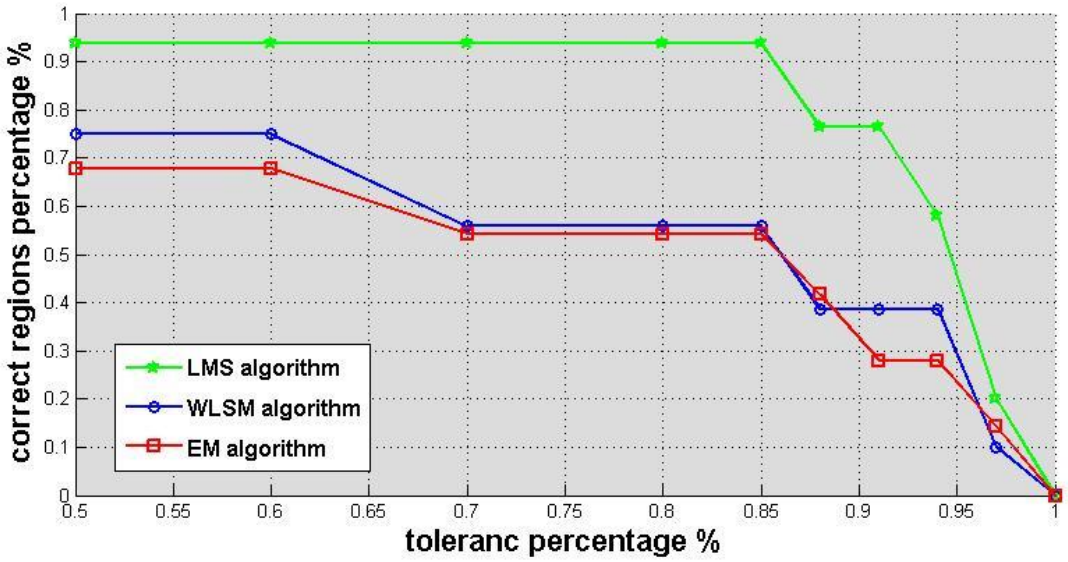

Fig. 6 Correct detection for EM, LSM and LMS.

6. Conclusion

Since LSM is based on minimizing the sample mean and these means are sensitive to extreme values, it makes sense that LMS, which replaces the mean by the much less sensitive median, will generate a more robust fitting method.

7. References

[1] University of South Florida Range Image Database, http://marathon.csee.usf.edu/range/DataBase.html

[2] Ballard, D.H. and C.M. Brown, "Computer vision", ed. N.J.P. Hall. 1982.

[3] M. E. Mortenson, "Geometric Modeling", New York, Chichester, Brisbane, Toronto, Singapore: John Wiley & Sons, 1985.

[4] Hoover, A., G. Jean-Baptiste, and X. Jiang., "An Experimental Comparison of Range Image Segmentation Algorithms". IEEE Trans, Pattern Analysis and Machine Intelligence, 1996. 18 (7): p. 673-689.

[5] Hussein S. Taha, "Extraction of 3D Object Representations from a Single Range Image", Faculty of the Virginia Polytechnic Institute and State University, Jan.5, 2000.

[6] O. D. Faugeras and M. Hebert. "A 3-D Recognition and positioning algorithm using geometrical matching between primitive surfaces", Proc. 8th Int. Joint Conf. Artificial Intelligence, pages 996-1002, IJCAI-83, August 1983.

[7] Iluud M. Bolle and David B. Cooper, "On Optimally Combining Pieces of Information, with Application to Estimating 3-D Complex-Object Position from Range Data". IEEE Transactions on Pattern Analysis and Machine Intelligence, PAMI-8:619-638, September 1986.

[8] Parameter Estimation and error Analysis of Range Data Prabhat K. Acharya Thomas C. Henderson Department of Computer Science University of Utah Salt Lake City, Utah 84112.

[9] R. Jain, R. Kasturi, and B. G. Schunk, Machine Vision, McGraw-Hill, New York, 1995.

[10] Barreto and Howland, "An Introduction to Least Median of Squares", Econometrics via Monte Carlo Simulation, July 24, 2001.

[11] Mount, David M., Nathan S. Netanyahu, Kathleen Romanik, Ruth Silverman, Angela Y. Wu, “A Practical Approximation Algorithm for the LMS Line Estimator,” 8th Ann. ACM-SIAM Symposium on Discrete Algorithms, 1997, 473-482.
[12] Rousseeuw, Peter J., “Least Median of Squares Regression”, Journal of the American Statistical Association, 79 (388) (1984), 871-880.
[13] A. Hoover et al., "A Methodology for Evaluating Range Image Segmentation Techniques", IEEE Workshop on Applications for Computer Vision (WACV), 1994.
[14] R. C. Gonzles, R. E. Woods, Digital Image Processing, Addison-Wesley, 1992.
[15] Gustavo Osorio, Pierre Boulanger and Flavio Prieto, “An Experimental Comparison of a Hierarchical Range Image Segmentation Algorithm”, Proceedings of the Second Canadian Conference on Computer and Robot Vision (CRV 2005).